16th Australasian Fluid Mechanics Conference
Crown Plaza, Gold Coast, Australia
2-7 December 2007

Droplets Transport in a Microfluidic Chip for *In Vitro* Compartmentalisation

Y. Zhu[1], M. N. Noui-Mehidi[1], P. W. Leech[2], B. A. Sexton[2], S. Brown[3], N. Wu[1,4] and C. Easton[4]

[1] CSIRO Materials Science and Engineering, PO Box 56, Highett, VIC 3190, AUSTRALIA

[2] CSIRO Materials Science and Engineering, Private Bag 33, Clayton South MDC, VIC 3169, AUSTRALIA

[3] CSIRO Entomology, GPO Box 1700, Acton, Canberra, ACT 2601, AUSTRALIA

[4] Research School of Chemistry, Australian National University, ACT 0200, AUSTRALIA

Abstract

In vitro compartmentalisation is an emerging technology for protein evolution and selection. In this presentation, we will report the development of a microdrop-based microfluidic platform for in vitro enzyme evolution and selection applications. A microfluidic chip has been developed and fabricated using the standard photolithography method in conjunction with electroplating and hot embossing techniques. A cross channel geometry was used to focus liquid flows for droplet generation. To realize on-chip compartmentalised bio-reactions, two droplet generators were fabricated on the same chip. Experiments have been carried out to measure droplet size, generation rate and speed using a photographic technique. Droplet size was found to be decreasing with increasing focusing oil flow rate for a given aqueous phase flow rate. When two droplet generators are used in the same chip, the droplets may be generated asynchronously due to different flow conditions. If the droplets were significantly smaller than channel size, the faster moving droplets could pass the slower moving droplets with little coalescence. If the droplets were of the channel size, the faster moving droplets would break or fuse with the slow droplets. To achieve high rate of droplet fusion, active control should be in place for synchronous generation and fusion.

Introduction

In vitro compartmentalisation (IVC) refers to cell-like compartments generated artificially as reaction chambers. In biology, cells use walls to confine networks of chemical reactions so that these reactions can not be messed up or easily disturbed by the outside world. This organisational model inspired Tawfik and Griffiths (1998[13]) to develop a system using micron-size water droplets dispersed in oil medium in which individual gene sequences could be contained with the enzyme variant they encode. The emulsion droplets in IVC can have a size ranging from a few microns to a few hundreds microns. The potential high capacity (more than 10^{10} drops per millilitre of sample) and ease of formation render it an ideal means of compartmentalising biochemical and genetic assays (Griffths and Tawfik 2006 [5]). Such a capacity can not be achieved in in conventional assays (a 10 μl assay in a 1536-well microtitre plate).

Although the IVC technology has only been developed recently, it has attracted a great deal of attention since the last few years. A number of review articles have been published such as Griffiths and Tawfik[4, 5], Amstuts et al, [1], Leamon et al. [8], Rothe et al.[11], Kelly et al.[7]. Recently, there has been a number of studies on the development of lab-on-a-chip technolgies for IVC applications (e.g. Link et al.[9], Huebner et al.[6]). Drop generation using microfluidics has proven to be more advantageous than conventional lab methods since it can produce monodisperse droplets with controlable sizes. In addition, microfluidic technologies can also provide means of droplet spliting, fusion, sorting and in-drop detection.

The Synthetic Enzymes initiative in CSIRO is a multi-institutional effort aiming to develop enzymes with dramatically shifted functions or mechanisms that are capable of catalysing novel reactions not known in nature. This will be achieved by developing technology to introduce novel chemical groups to enzymes to synthesise enzymes using highly controllable cell-free methods, and to evolve enzymes using IVC technology. This paper will report some of the results in the IVC chip development. In particular, we will present some of the data on behaviour of droplets transport in microchannels.

Chip design and fabrication

The two commonly used methods for on-chip drop generation include a T-junction channel network (e.g. Nisisako et al.[10]) and a cross-junction (e.g. Anna et al.[2]). In the latter case, the flow is focused by the two side channels to form droplets. This method was used in the present study. A picture of the microchip is shown in Figure 1.

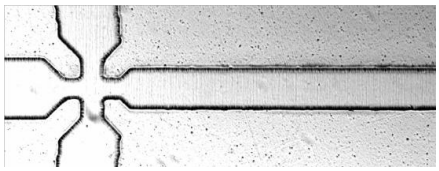

Figure 1: A picutre of the fabricated droplet chip. The channel width is 115 μm at the nozzle and 207 μm at the main section.

The microchip was fabricated in a polycarbonate slide with dimensions of $75mm \times 25mm$ and a thickness of $2mm$. The microchip was fabricated in the CSIRO Microfabrication Laboratory, Clayton, VIC 3169, Australia. The microfluidic channel pattern was designed using a commercial layout tool and fabricated as a film mask. The mask pattern was exposed into a 70 μm layer of Laminar 5083 resist/stainless steel plate using a collimated UV exposure system. The exposed pattern was developed in a Na_2CO_3 solution and the resulting profile was replicated as a nickel shim by a two-stage process. Firstly, a thin layer of nickel was sputter deposited onto the patterned surface followed by a thicker electrodeposited layer (100 μm) in a nickel sulphamate bath. The nickel shim was subsequently used as a die to hot emboss the pattern of channels into polycarbonate chips. The embossing was performed in a planar hydraulic press at a temperature of $155°C$. During embossing, the pressure was maintained for two minutes and then released after cooling to $50°C$. The access holes were then drilled through the backside of the polycarbonate plate. Before laminating the capping layer, the polycarbonate chip was treated with oxygen plasma for 15 minutes. To access the microchannels in the chip, a nano-ports assembly was carefully glued to each liquid port.

Experimental Details

The droplet experiments were carried out in the CSIRO Microfluidics Laboratory at Highett, Melbourne, Australia. To produce water-in-oil droplets, the water solution was pumped from the left-hand side of the horizontal channel (Figure 2) while the oil solution was pumped simutaneously from the two inlets in the side channels.

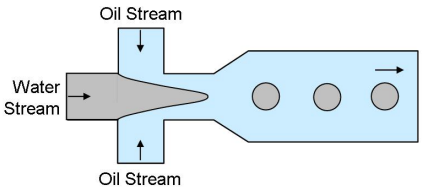

Figure 2: A sketch of drop formation principle.

The symmetric oil branches and the water branch intersected at the inlet of the production channel which was directed towards downstream processing or waste. Droplets were formed when the aqueous jet breaks due to the shear force by the oil streams. The oil and water channels each had a width section of 315 μm which decreased to 115 μm at the junction point. The production channel had a width of 207 μm and all channels had the same depth of 70 μm. The cross section of each channel was rectangular. In the present study, deionised water was used for the aqueous phase while ETA oil was used as the organic phase. The ETA vegetable oil was manufactured by Goodman Fielder Food Services Limited, Australia. The kinematic viscosity of the oil phase is 15.4 mPaS at 20C and a density of 975 kg/m^3 while the aqueous phase has a density of 1000 kg/m^3 and a kinematic viscosity of 1 mPaS. The interfacial tension between the oil and the water phase has been reported as 0.033 N/m. Both the water and oil streams were generated by the use of two identical Razel A-99 syringe-pumps equipped with Terumo syringes of 5 ml capacity. The syringes were fitted with high grade filters in order to eliminate any potential microscopic contaminant in each of the phases. Droplet formation at the junction point was monitored visually by a Nikon Eclipse TE2000-U microscope and a video camera Basler A 6021C-2 equipped with a Nikon C-0.45× demagnification lens. The camera was capable of capturing images at a frequency of 30 frames per second. The experimental setup is shown in Figure 3.

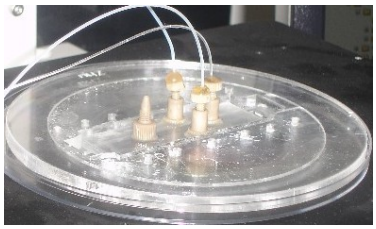

Figure 3: Experimental set-up for droplet generation and control. The droplet chip was placed in a chip holder with liquid and electreical interface for liquid and electrical current deliveries.

The interfacial tension between the walls and the oil phase was lower than that between the walls and the dispersed water phase, stable water-in-oil (W/O) droplets could be formed in the current conditions. Initially the channels were completely filled with the oil phase using the lowest flow rate before commencement of the water stream. The flow rate in the water stream was gradually increased until the observation of droplets. The lowest flow rates at which droplet could be generated were 0.031 ml/h and 0.095 ml/h for the water phase and oil phase, respectively. The effect of the continuous flow rate on the droplet size was then investigated by increasing the oil flow rate gradually. A sequence of pictures captured from the video camera was saved to a computer for each oil flow rate in order to process digitally the images. The droplet size was measured by image processing of the recorded frame. The size of droplets was averaged over a batch of consecutive images captured for specific water and oil flow rates. The water flow rate was fixed to 0.031 ml/h and the oil flow rate was increased from 0.095 ml/h to 0.955 ml/h.

Results

Drop generation by flow focusing

In Figure 4, a series of sample images show a typical decrease of water droplet size when the flow rate of the continuous oil stream was increased. The two oil streams which intersected laterally acted to shear off the water jet formed at the entrance of the junction. With increase in flow rate of the oil, it can be seen from the images that the water jet tip became sharper and very fine droplets could be regularly generated.

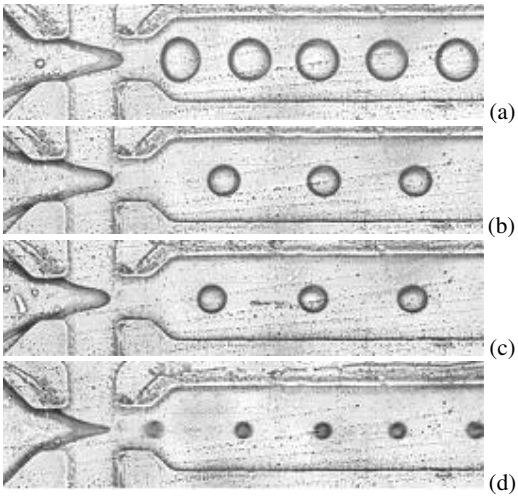

Figure 4: Visualization of the droplet generation in the microfluidic chip under different flow conditions. The water flow rate Q_w was 0.031 ml/h. The main channel had a width of 207μm and a height of 70μm. The oil flow rates were 0.096, 0.287, 0.446 and 0.955 ml/h for cases (a) to (d), respectively.

The analysis of the images has shown that the average droplet size, d, decreased monotonically with increasing oil flow rate Q_o as seen in Figure 5. From the study by GI Taylor[14], the drop formation is a result of the shearing force applied by the oil streams on the water stream at the junction. The predicted droplet size d is proportional to $\sigma/\mu\gamma$, where σ is the interfacial tension, μ is the continuous phase viscosity and γ is the shear rate. For a nozzle size of D and a flow rate of the continuous phase Q_o, γ is proportional to Q_o/D^3. Therefore the drop size should depend on the flow rate inversely(e.g. Cristini and Tan[3]), via,

$$d \propto \frac{\sigma D^3}{\mu Q_o}. \quad (1)$$

The dependence of drop size on the oil flow rate is shown in Figure 5. The drop size was normalised by the nozzle size d while the oil flow rate was non-dimensionalised by the water flow rate Q_w. Also plotted in the figure are data obtained by Tan et al.[12] for three differentQ_w cases. All the data seem to indicate that when the flow ratio was greater than about 15, the slope of the drop size is close to 1 from Eq. 1, implying that the shearing force was the main mechanim for drop generation. From the theoretical study by Tomotika [15], for a viscosity ratio (μ_w/μ_o) of 0.065, the drop formation wavelength should be around $5.7d$ or $220\mu m$ for case (d) of Figure 4, in which the flow ratio is about 15. This value agrees reasonably with the drop spacing of 200 μm measured from the picture. However, for smaller ratio values, the slope deviates significantly from that of Eq. 1.

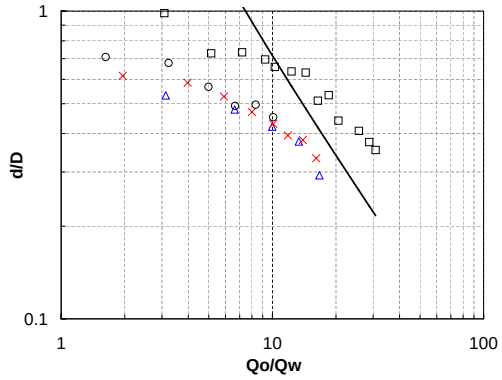

Figure 5: Variation of droplet size as a function of the oil phase flow rate. The acqueous phase flow rate was constant at 0.031 ml/h. The lines indicate the slope implied from Eq. 1 and the magnitudes were arbitrarily adjusted for clarity of comparison. Current measurement: □; Measurement by Tan et al.[12]: Q_w = 0.3 (△), 0.5 (×) and 0.6 $\mu l/min$ (○), respectively. $D = 48\mu m$.

Double droplet streams

When two streams of droplets are required, two generators can be arranged in the same chip as shown in (Figure 6). The two droplets streams may be produced independently from each nozzle. If the flow conditions were identically and material conditions were appropriate, the two drops could collide and merge into one large drop.

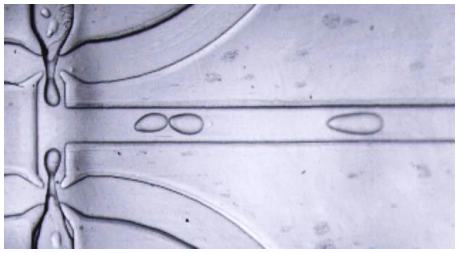

Figure 6: A picture of the droplet chip with two streams of droplets generated and fused in the main channel.

However, if the droplets produced were too small, the drops might flow side by side without contact as in Figure 7. Further, if the flow conditions were slightly different between the two nozzles, the two streams of droplets were produced asynchronously, possibly with different size and rate. In this situation, the two droplets had little chance of coalescence near the T-junction except for cases where the two droplets happened to be very colse to each other.

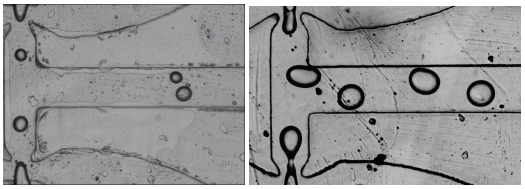

(a) (b)

Figure 7: Images of droplets generated from the two nozzles (a) synchronous generation (b) asynchronous generation. No fusion observed.

In the asynchronous mode, if the drop generation rates and droplets sizes from the two nozzles are different, the speed of droplets movement may be different too. This is revealed in Figure 8 in which a series of consecutuve images were taken from two droplet streams. One stream of droplets were water doped with fluorescence dye (white droplets) while the other contained water only (dark drolets). It is clear from the images that the white droplets travelled at a faster rate and squeezed through the gap between the drop and channel walls. It was observed that the coalescence rate was very low during the passing. This was probably due to the fact that the droplets were relatively small and the gap was large so that the second droplet could squeeze through without much time for contact. In the second experiment where droplets of the channel size were formed, the gap was smaller and the faster droplets could not squeeze through easily. The droplets broke into two and each half squeesed through the gap on each side of the channel separately. The smaller droplet would then remain closer contact with the front droplet and subsequently coalescence was observed. This process is highlighted by the boxes in Figure 9.

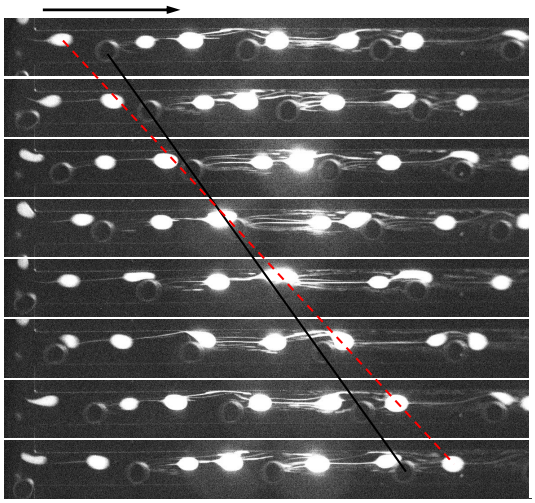

Figure 8: A series of images showing one stream of drops passing another stream of drops in the main channel of the chip. The arrow indicates direction of flow. The solid and the broken lines mark the locations of the white and dark droplets, respectively. The time between images were 60.6ms.

Figure 10 shows the results from image analysis of Figure 8. The white droplets traveled at a velocity of 7.45mm/s (±5%). The oil phase flow rate was 300 μl/h, which corresponds to a mean velocity of the carrier liquid of 7.7 mm/s. The white drops moved slightly slower than the bulk oil phase due to the friction

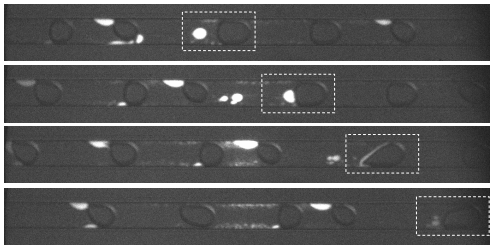

Figure 9: A series of images showing passive droplet fusion. The time between images were approximately 149ms. The boxes highlight the droplets of interest.

and drag forces. The velocity of the dark drops was 5.4 mm/s (uncertainty ±5%). The difference between the two streams of drops was perhaps due to the difference in the two aqueous streams since the flow rates were 57 and 62 μl/h for the dyes and normal streams, respectively. The drop generation rate was therefore different. Results from images taken 20mm from the cross section were consistent with those taken near the cross section, thus ruling out effect of the slight difference in the oil flow rates of each nozzle. It is recommended that more active control of the drop size and movement be required in order to keep track of individual drops of interest in sequence.

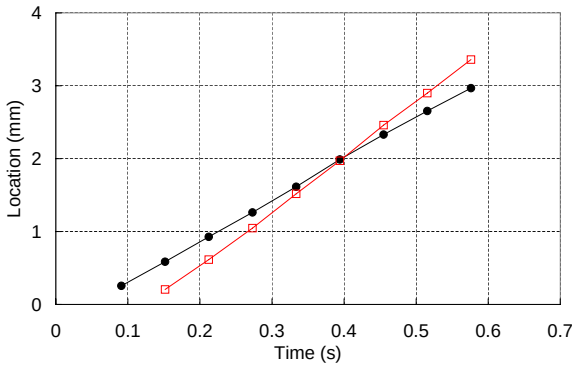

Figure 10: Centre postions of two drops as a fucntion of time. Positions measured from the start of the main channel.

Conclusions

The experimental investigations on droplet generation and transport in microfluidic channels have been carried out. The microfluidic chip was made of polycarbonate and fabricated in CSIRO. The droplets were generated by flow focusing method and the channel size at the nozzle was 115μm. With the present oil-water system, the droplet size decreased with increasing oil flow rate for a given water flow speed. The drop sizes varied from 40 to 103 μm. In the case of two-nozzle system, two streams of droplets could be be produced independently. For identical nozzle flow condtions, the two streams could be generated synchronously and brought together for fusion. For different nozzle flow conditions, the droplet generations from the two nozzle was asynchronous with different drop generation rate. If the droplets were significantly smaller than channel size, the faster moving droplets could pass the slower moving droplets with little coalescence. If the droplets were of the channel size, the faster moving droplets would break or fuse with the slow droplets. To achieve high rate of droplet fusion, active control should be in place for synchronous generation and fusion.

References

[1] Amstutz, P., Forrer, P., Zahnd, C. and Plückthun, A., In vitro display technologies: Novel developments and applications, *Curr Opin Biotech*, **12**, 2001, 400–405.

[2] Anna, S. L., Bontoux, N. and Stone, H. A., Formation of dispersions using flow focusing in microchannels, *App. Phys. Lett.*, **82**, 2003, 364–366.

[3] Cristini, V. and Tan, Y.-C., Theory and numerical simulation of droplet dynamics in complex flows-a review, *Lab on a Chip*, **4**, 2004, 257–264.

[4] Griffiths, A. D. and Tawfik, D. S., Man-made enzymes from design to in vitro compartmentalisation, *Curr. Opin. Biotech.*, **11**, 2000, 338–353.

[5] Griffiths, A. D. and Tawfik, D. S., Miniaturising the laboratory in emulsion droplets, *Trends in Biotech.*, **24**, 2006, 395–402.

[6] Huebner, A., Srisa-Art, M., Holt, D., Abell, C., Hollfelder, F., DeMello, A. J. and Edel, J. B., Quantitative detection of protein expression in single cells using droplet microfluidics, *Chem Comm*, 1218–1220.

[7] Kelly, B. T., Baret, J.-C., Taly, V. and Griffiths, A. D., Miniaturizing chemistry and biology in microdroplets, *Chem. Commun.*, 1773–1788.

[8] Leamon, L. H., Link, D. R., Egholm, M. and Rothberg, J. M., Overview: Methods and applications for droplet compartmentalization of biology, *Nature Methods*, **3**, 2006, 541–543.

[9] Link, D. R., Grasland-Mongrain, E., Duri, A., Sarrazin, F., Cheng, Z., Cristobal, G., Marquez, M. and A.Weitz, D., Electric control of droplets in microfluidic devices, *Angew. Chem. Int. Ed.*, **45**, 2006, 2556–2560.

[10] Nisisako, T., Torii, T. and Higuchi, T., Droplet formation in a microchannel network, *Lab on a Chip*, **2**, 2002, 24–26.

[11] Rothe, A., Surjadi, R. N. and Power, B. E., Novel proteins in emulsions using in vitro compartmentalization, *Trends Biotech.*, **24**, 2006, 587–592.

[12] Tan, Y.-C., Cristini, V. and Lee, A. P., Monodispersed microfluidic droplet generation by shear focusing microfluidic device, *Sensors and Actuators B*, **114**, 2006, 350–356.

[13] Tawfik, D. and Griffiths, A., Man-made cell-like compartments for molecular evolution, *Nat. Biotechnol.*, **16**, 1998, 652–656.

[14] Taylor, G. I., The formation of emulsions in definable fields of flow, *Proc. Roy. Soc. Lond. A*, **146**, 1934, 501–523.

[15] Tomotika, S., On the instability of a cylindrical thread of a viscous liquid surrounded by another viscous fluid, *Proc. Roy. Soc. Lond. A*, **CL**, 1935, 322–337.